英文版教材

DIAGNOSTIC IMAGING

诊断影像学

·第2版·

主　编　刘林祥

人民軍醫出版社
PEOPLE'S MILITARY MEDICAL PRESS

R445
92-2

英文版教材

DIAGNOSTIC IMAGING

诊断影像学

（第2版）

主　编　刘林祥

副主编　童国礼　张　晶
　　徐　凯　张　玫

中医学院　0669867

PEOPLE'S MILITARY MEDICAL PRESS

北　京

图书在版编目（CIP）数据

诊断影像学/刘林祥主编. —2版. —北京：人民军医出版社，2012. 8
ISBN 978-7-5091-5927-9

Ⅰ.①诊… Ⅱ.①刘… Ⅲ.①影像诊断—医学院校—教材 Ⅳ.①R445

中国版本图书馆CIP数据核字（2012）第177097号

策划编辑：程晓红　**文字编辑：**陈　杰　**责任审读：**陈晓平
出版发行：人民军医出版社　**经销：**新华书店
通信地址：北京市100036信箱188分箱　**邮编：**100036
质量反馈电话：（010）51927290；（010）51927283
邮购电话：（010）51927252
策划编辑电话：（010）51927300—8718
网址：www. pmmp. com. cn

印、装：三河市春园印刷有限公司
开本：787mm×1092mm　1/16
印张：20.25　**字数：**860千字
版、印次：2012年8月第2版第1次印刷
印数：0001—3000
定价：65.00元

版权所有　侵权必究
购买本社图书，凡有缺、倒、脱页者，本社负责调换

内容提要 Summary

本书为诊断影像学英文版教材，共9章，包括影像基本技术、颅脑、骨与关节、肺纵隔、循环系统、消化道、肝胆胰脾、泌尿器官、盆腔生殖器官，突出各系统常用、最新影像检查技术，重点介绍常见病、多发病的典型图像，并在每章后加入英汉词汇，便于读者学习、检索。本书形式新颖、图文并茂、信息量大，可作为医学院校医学影像学专业英语教材，也可作为医学影像与核医学专业研究生的专业参考读物。

编著者名单

（以姓氏笔画为序）

于广会　泰山医学院放射学院

马芳芳　泰山医学院放射学院

马奎元　济宁医学院

王永栋　加拿大 McMaster 大学

王海燕　山东省医学影像学研究所

卢　川　泰山医学院放射学院

刘玉金　上海市第十人民医院

刘林祥　泰山医学院放射学院

孙庆举　山东省省立医院

杜　勇　川北医学院

李长勤　泰山医学院附属医院

张　玫　泰山医学院放射学院

张　林　滨州医学院附属医院

张　晶　牡丹江医学院医学影像学院

林岳兴　广州医学院第二临床学院

徐　凯　徐州医学院医学影像学院

董　鹏　潍坊医学院

童国礼　川北医学院

此为试读，需要完整PDF请访问：www.ertongbook.com

再版前言 Preface

为培养面向世界、面向现代化、面向未来的医学影像学专业高素质人才，适应医学影像学英语教学的需要，编者在原自编专业英语阅读教材的基础上，整理、编集了部分医学影像学的英文内容，2006年编写出版了《诊断影像学（英文版）》一书，以配合医学影像学规划教材作为医学院校临床医学专业医学影像学和医学影像学专业医学影像诊断学的专业英语和双语教学的辅助教材，也作为研究生的医学影像学参考读物。通过本书的学习和阅读，达到熟悉医学影像诊断常用英文词汇的目的，为阅读英文专业书刊奠定基础。应用于教学以来，得到了读者的支持，收到了许多有益的建议。

在本书再版修订中，根据授课教师在教学应用过程中反馈的意见和建议，删减多数表格，改为文字叙述；对部分章节进行了删减；更换了部分典型图片，以期更适于教师的教学和读者的学习。

本书再版过程中得到了参与编写院校专业教师的热情支持，很多学生和研究生读者也提出了不少建议，使本书不断完善，再次谨致衷心的感谢。

医学影像学发展迅速，再版修订中，虽然各位编者尽心尽力，但由于专业知识水平所限，书中缺点和错误在所难免，恳请广大教师、同学和读者不吝赐教。

刘林祥

2012年6月

目 录 Contents

Chapter One Imaging Technique / 1

Chapter Two Brain / 10

Chapter Three Bone and Arthrosis / 58

Chapter Four Lungs, Mediastinum and Breast / 105

Chapter Five Circulatory System / 166

Chapter Six Digestive Tract / 203

Chapter Seven Liver, Biliary, Pancreas and Spleen / 224

Chapter Eight Urinary System and Adrenal Gland / 276

Chapter Nine Pelvis and Genital Organ / 298

Chapter One

Imaging Technique

1 Multislice Computerized Tomography

Multislice Computerized Tomography (MSCT) is a recent development in CT technology where the linear array of detector elements used in typical conventional and helical CT scanners has been replaced by a two-dimensional array of detector elements (Fig. 1-1). Using the detector array, MSCT scanners can acquire multiple slices or sections simultaneously and thereby greatly increase the speed of CT image acquisition. In the single section CT scanner, the shape of each detector element facing the X-ray beam is a rectangle (about 1mm×20mm) as shown (Fig. 1-2). While scanning, the entire detector element is actively detecting radiation, and the slice thickness is controlled by the width of the collimation of the X-ray beam (Fig. 1-3). In the MSCT scanner, the two-dimensional detector array is divided into smaller elements. In the example shown, the long dimension (20 mm) of the single section CT detector element is divided into 16 elements of 1.25 mm each. In the first release of the MSCT scanners, all vendors provided for the acquisition of four slices simultaneously. To allow for variation in the width of the slices, the signals from multiple rows of detector elements are combined. In the example shown in the bottom of Figure 2, pairs of rows are combined together giving 4 slices that are about 2.5 mm each and the X-ray beam is collimated to cover the full 8 rows of the detector array.

Two types of detector arrays were introduced with the development of MSCT fixed and adaptive arrays. In the fixed array detector, the sub-elements are all the same width (Fig. 1-2, Fig. 1-3), and the slice thickness is varied by changing the number of rows which are combined together for form the acquired sections. It is technically possible to acquire two very thin slices of about 0.5 mm, or four slices of 1.25 mm, 2.5 mm, 3.75 mm and 5.0 mm. In the adaptive array detector (Fig. 1-4), the outer elements are proportionately larger, and the detector allows the acquisition of two 0.5 mm slices and four slices of 1.0 mm, 2.5 mm, and 5.0 mm (Fig. 1-5, Fig. 1-6).

Image reconstruction in MSCT is more complicated than that in single section CT. When the table is stationary during image acquisition, the X-ray source and area detector are seen to form a cone projection. The measurements for any of the slices are not co-planar, and

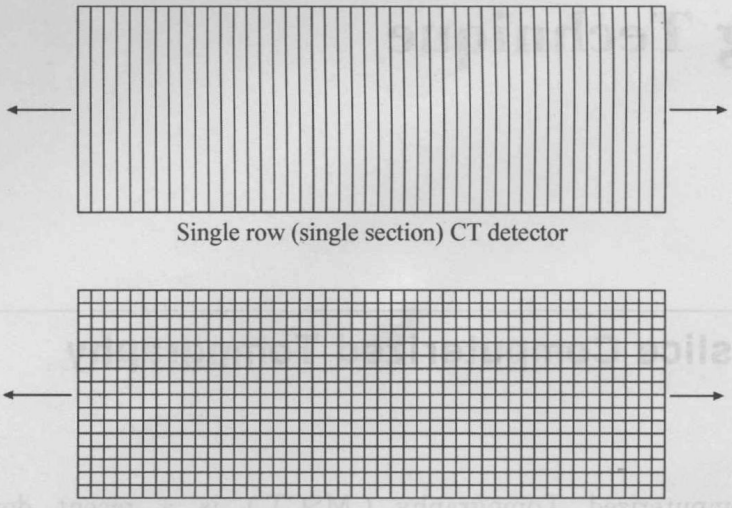

Fig. 1-1 MSCT Single section CT detector (top). Each detector element is about 1mm wide by 20 mm high. MSCT detector (bottom). The single section CT detector is replaced by multiple elements

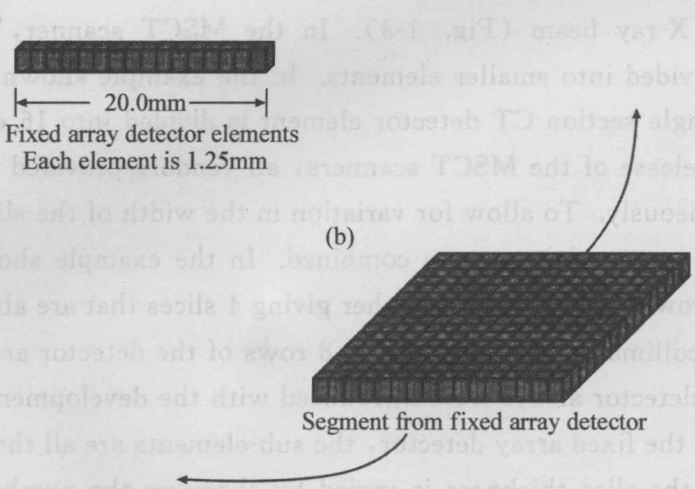

Fig. 1-2 MSCT Fixed array MSCT detector. (a) Single column of elements. The 20 mm length of the single section CT detector has been divided into 16 equal segments of 1. 25 mm each. (b) The columns of the fixed array detector are packed together to form a curved 2D detector array

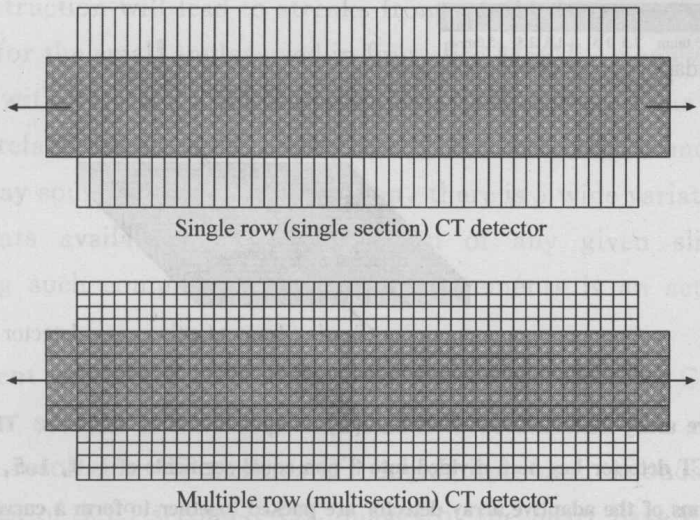

Fig. 1-3 MSCT Example of slice thickness control. In the single section CT detector (top), the slice thickness is totally controlled by the X-ray beam collimation. With the MSCT detector (bottom), slice thickness is controlled by the width of the X-ray beam collimation, the number of rows of the multislice detector that are selected and the reconstruction algorithm

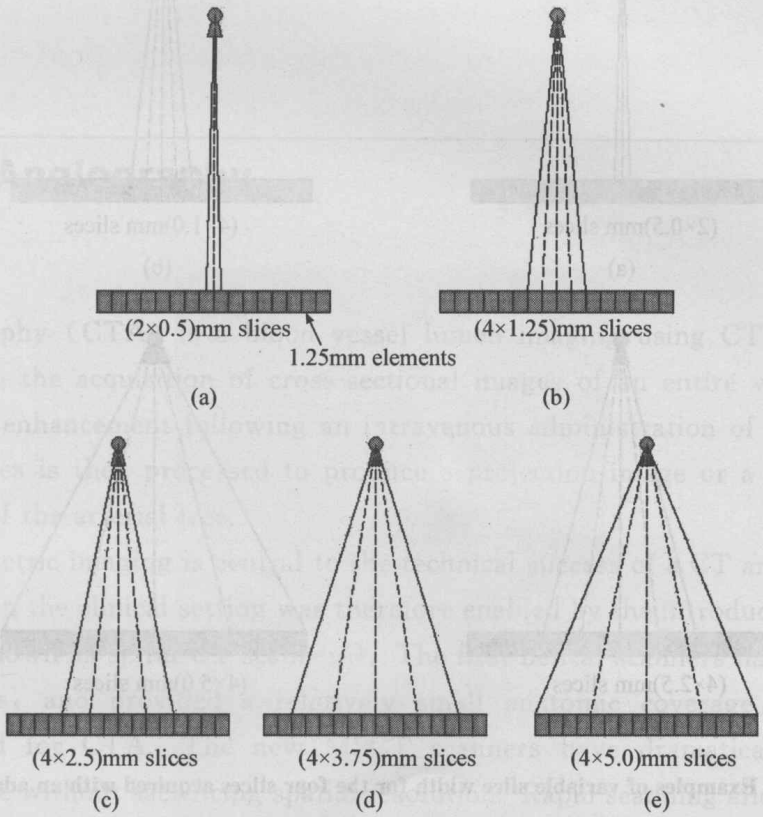

Fig. 1-4 MSCT Examples of variable slice width for the four slices acquired with a fixed width multislice CT detector. (a) The two central detectors are irradiated with a fraction of the X-ray beam forming two 0.5 mm slices. For the remaining figures (b-e), the beam width is increased to produce four slices, and the slices are combined in groups of 1, 2, 3 and 4 rows to give slice widths of (b) 1.25 mm, (c) 2.5 mm, (d) 3.75 mm, and (e) 5.0 mm

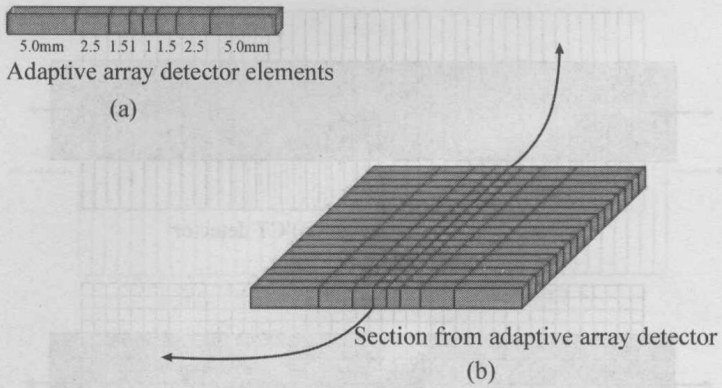

Fig. 1-5 MSCT Adaptive array multislice CT detector. (a) Single column of elements. The 20 mm length of the single section CT detector has been divided into 8 non-equal segments of 1.0, 1.5, 2.5 and 5.0 mm each. (b) The columns of the adaptive array detector are packed together to form a curved 2D detector array

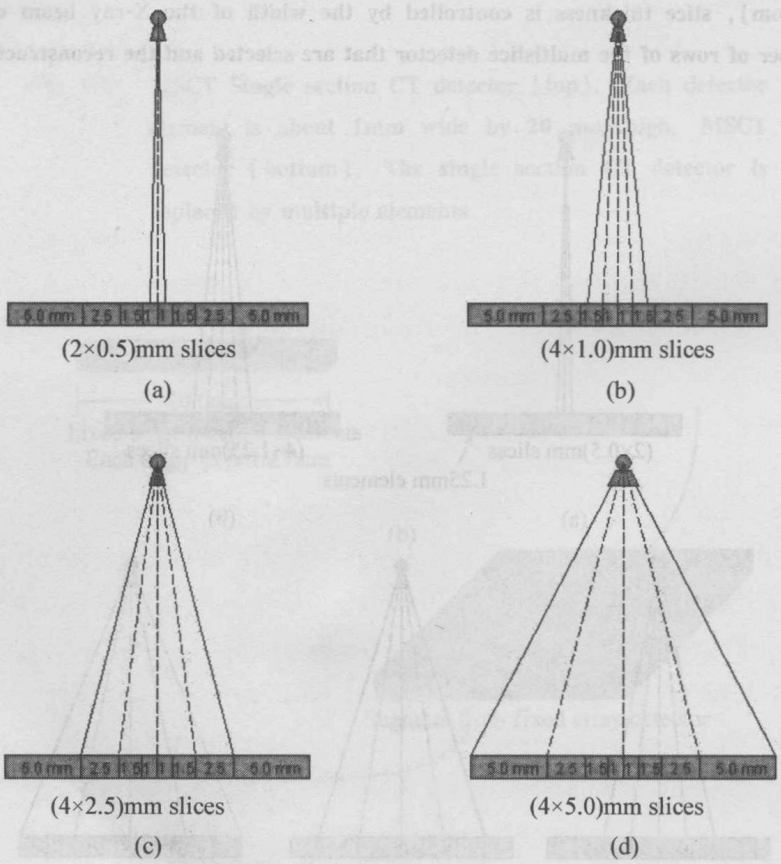

Fig. 1-6 MSCT Examples of variable slice width for the four slices acquired with an adaptive multislice CT detector. (a) The two central detectors are irradiated with a fraction of the X-ray beam forming two 0.5 mm slices. For the remaining figures (b-d), the beam width is increased to produce four slices, and the slices are combined to give slice widths of (b) 1.0 mm, (c) 2.5 mm, and (d) 5.0 mm

此为试读，需要完整PDF请访问：www.ertongbook.com

conventional reconstruction will lead to streaks from small, dense, points and edges. These artefacts are small for the small angles used in four slice MSCT. However, as the number of slices will increase with new technical improvements, the width of the cone angle will also increase and the artefacts may not be negligible. When the table is moved continuously in synchrony with X-ray source and detector rotation, there is a wide variation in the angulation of the measurements available for reconstruction of any given slice location. Image reconstruction using such complicated sets of measurements is an active area of ongoing research.

The development of MSCT has opened a new dimension to CT technology. The introduction of four slice simultaneous acquisition has allowed the development of new possibilities in high resolution CT such as CT angiography and colonoscopy. Coupled with half acquisition times of 0. 25 seconds, CT images of the heart have become possible. All manufactures are moving beyond four slice imaging to eight, sixteen and even greater numbers of slices. Although such scanners will be more expensive, the greatest component of the cost will be in the digital electronics which will continue to increase in power and decrease in cost for the foreseeable future.

2 CT Angiography

CT angiography (CTA) is a blood vessel lumen imaging using CT data. Typically, CTA begins with the acquisition of cross-sectional images of an entire volume during the arterial phase of enhancement following an intravenous administration of a contrast agent. The stack of slices is then processed to produce a projection image or a three-dimensional (3D) rendering of the arterial tree.

Rapid volumetric imaging is central to the technical success of a CT angiography study. CT angiography in the clinical setting was therefore enabled by the introduction of helical CT scanners (also known as spiral CT scanners). The first helical scanners had only one row of detector elements, and provided a relatively small anatomic coverage with the spatial resolution needed for CTA. The new MSCT scanners have dramatically increased the anatomic coverage without sacrificing spatial resolution. Rapid scanning allows the volume of interest to be imaged during uniform arterial enhancement and prior to venous enhancement. In addition, rapid imaging may allow more rapid infusion of contrast and therefore a higher contrast between the vessel lumen and the surrounding tissues.

Timing of the data acquisition with respect to the contrast administration is also important. The optimal delay between infusion and scanning can be patient dependent,

especially in subjects with poor cardiac output or vascular disease. While the delay is generally selected based on clinical experience, the optimal timing for a particular patient can be measured using a test injection during repeated scanning of a single section in the volume of interest. Automated techniques are also available; with these, the attenuation number is measured continuously in a vessel of interest, and when the attenuation has increased to a predetermined value, scanning is started automatically (after a small delay to allow for breath-hold instructions).

Viewing of single sections is tedious since a single study may involve hundreds of slices. In addition, appreciation of the continuity of vessels can be difficult when images are viewed in this mode. Therefore, simultaneous evaluation of the data for an entire volume is essential to proper and efficient image analysis. Several three-dimensional rendering (TE) techniques are available for CTA. Until recently, surface rendering and maximum intensity projection (MIP) were the most commonly used algorithms with CTA. Surface rendering is the least accurate technique of the two. MIP is extensively used in magnetic resonance angiography (MRA), but CT data is less well suited for MIP than magnetic resonance (MR) data because in CT there are likely to be non-vascular structures (*e. g.* bones and calcifications) with higher CT numbers than the vessel lumen. Spatial editing (manual, semiautomatic, or automatic) can be used to remove potentially confusing structures prior to MIP processing (Fig. 1-7). Today, volume rendering has become the algorithm of choice for CTA. Volume rendering renders the entire volume of data and obviates the tedious editing often necessary with MIP.

Because of its use of intravenous contrast administration, CTA is less invasive than

Fig. 1-7 CT angiography MIP projection of abdominal aortic aneurysm. Bone (vertebral column, pelvis) has been edited away

conventional angiography. It is also far more rapid (a typical exam might take only 15 minutes) and much less expensive. An additional advantage that should not be overlooked is that the CT images provide 3D information, for example of plaque morphology, they can help unravel overlapping structures, and they also provide soft tissue information. However, CTA does not provide the level of in-plane spatial resolution that conventional angiography achieves. As compared to MRA, CTA is more widely available and probably more robust, at least as compared to MR techniques that do not use contrast agents. Drawbacks of CTA as compared to MRA are use of ionizing radiation and iodinated contrast media which contrary to the gadolinium-containing MR contrast media, are potentially nephrotoxic.

3 Cerebral Angiography

Despite the advances of CT angiography, MRA, and Doppler ultrasound techniques, there are still numerous indications for angiography of the supra-aortic branches. However, many of the indications are connected to the possibility of catheter interventions such as embolization, percutaneous transluminal angioplasty (PTA) and stenting, and local thrombolysis.

The main indications for cerebral angiography are: a) stenosis and occlusion, b) aneurysms of the neck vessels and intracerebral arteries, c) arteriovenous malformations (AVM) and fistulae (AVF), and d) highly vascular extra- and intracranial tumors (meningioma, glomus tumor, angiofibroma).

Cerebral angiography may be performed as non-selective arch angiography to demonstrate the origin of the supra-aortic branches. This method may also serve to evaluate atherosclerotic lesions at the carotid bifurcation [Fig. 1-8 (a)]. Selective cerebral angiography is divided into carotid and vertebral arteriography.

Carotid arteriography is today routinely performed via a percutaneous femoral approach using preformed catheters (headhunter etc.). According to the indication and suspected lesion, the common carotid artery [Fig. 1-8 (b)] or the internal and external carotid arteries are injected super-selectively. Alternatively, the right carotid artery may be visualized by retrograde filling of the subclavian artery via a transbrachial approach (counterflow angiography). On the left the same method will show the left vertebral artery. Direct carotid puncture today is practically obsolete.

Vertebral arteriography is also performed via a transfemoral approach, or alternatively the less risky counterflow injection via uni- or bilateral brachial approach may be used. Indications for vertebral arteriography are investigation of lesions of the vertebral arteries,

the cerebellar arteries, the basilar artery, the posterior cerebral arteries and the function of the circle of Willis.

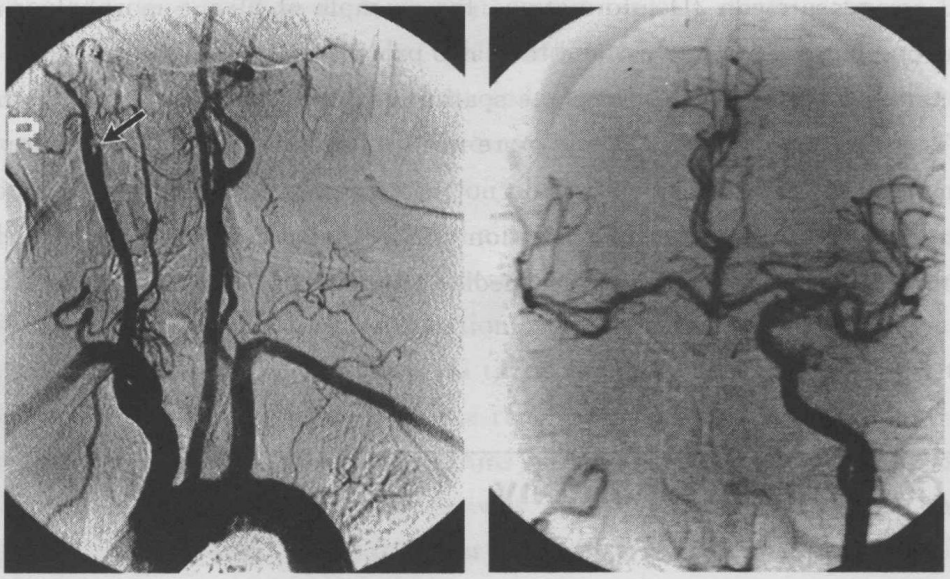

(a) (b)

Fig. 1-8 Cerebral angiography Injection of the aortic arch (a) demonstrates the supraaortic branches. Note occlusion of right internal carotid artery (arrow). Selective injection of left carotid artery (b) in same patient shows cross filling of right anterior and middle cerebral artery across the anterior communicating artery

Vocabulary

array [ə'rei]	*n.* 阵列
rectangle ['rektæŋgl]	*n.* 矩形
helical ['helikəl]	*adj.* 螺旋形的，螺旋线的
collimation [ˌkɔli'meiʃən]	*n.* 瞄准，调整
algorithm ['ælgəriðəm]	*n.* 运算法则，算法

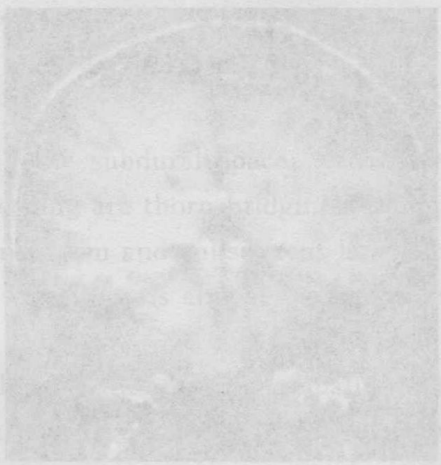

Chapter Two

Brain

1 Intracranial Hematoma

(1) Epidural hematoma

Epidural hematoma is an extra cerebral blood collection, located between the dura and the inner table of the skull. Usually arterial, the lesion is almost invariably post-traumatic and associated with a skull fracture and tearing of the meningeal vessels. An epidural hematoma may result from a tear of the dural sinus and then be venous in origin (Fig. 2-1). This type of hematoma is more common in the posterior fossa and results from a tear of the transverse or sigmoid sinus.

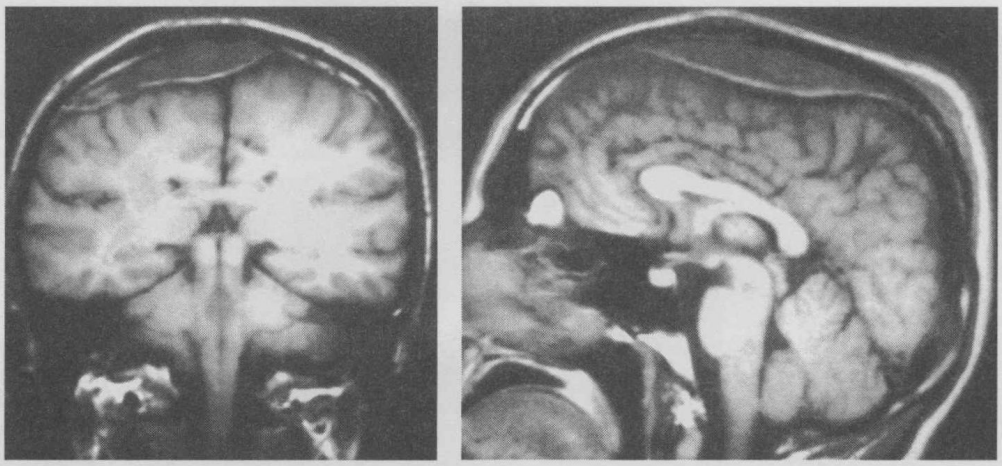

(a) (b)

Fig. 2-1 Epidural hematoma T_1WI in coronal (a) and sagittal (b) planes of a venous epidural hematoma due to tear of the superior sagittal sinus following a fracture of the parietal bone at the vertex. The hematoma crosses the midline, the dura and the sinuses are detached from the inner table and displaced downward

The shape is usually biconvex and not crescentic, unlike the majority of subdural hematomas.

An epidural hematoma, frontal, occipital or at the vertex, may cross the midline;

此为试读，需要完整PDF请访问：www.ertongbook.com